UCRL-ID-144840

Advanced Imaging Catheter: Final Project Report

P. Krulevitch, B. Colston, L. DaSilva, D. Hilken, J-U Kluiwstra, A. P. Lee, R. London, R. Miles, D. Schumann, K. Seward, A. Wang

July 20, 2001

U.S. Department of Energy

Lawrence Livermore National Laboratory

DISCLAIMER

This work was performed under the auspices of the U. S. Department of Energy by the University of California, Lawrence Livermore National Laboratory under Contract No. W-7405-Eng-48.

Advanced Imaging Catheter: Final Project Report

P. Krulevitch, B. Colston, L. DaSilva, D. Hilken, Jan-Ulco Kluiwstra, A.P. Lee, R. London, R. Miles, D. Schumann, K. Seward, and A. Wang

Introduction

Minimally invasive surgery (MIS) is an approach whereby procedures conventionally performed with large and potentially traumatic incisions are replaced by several tiny incisions through which specialized instruments are inserted. Early MIS, often called laparoscopic surgery, used video cameras and laparoscopes to visualize and control the medical devices, which were typically cutting or stapling tools. More recently, catheter-based procedures have become a fast growing sector of all surgeries. In these procedures, small incisions are made into one of the main arteries (e.g. femoral artery in the thigh), and a long thin hollow tube is inserted and positioned near the target area. The key advantage of this technique is that recovery time can be reduced from months to a matter of days. In the United States, over 700,000 catheter procedures are performed annually representing a market of over $350 million. Further growth in this area will require significant improvements in the current catheter technology.

In order to effectively navigate a catheter through the tortuous vessels of the body, two capabilities must exist: imaging and positioning. In most cases, catheter procedures rely on radiography for visualization and manual manipulation for positioning of the device. Radiography provides two-dimensional, global images of the vasculature and cannot be used continuously due to radiation exposure to both the patient and physician. Intra-vascular ultrasound devices are available for continuous local imaging at the catheter tip, but these devices cannot be used simultaneously with therapeutic devices. Catheters are highly compliant devices, and manipulating the catheter is similar to pushing on a string. Often, a guide wire is used to help position the catheter, but this procedure has its own set of problems. Three characteristics are used to describe catheter maneuverability:

- pushability -- the amount of linear displacement of the distal end (inside body) relative to an applied displacement of the proximal end (outside body).
- torquability -- the amount of rotation of the distal end relative to an applied rotation of the proximal end
- trackability -- the extent to which the catheter tracks along the guide wire without displacing it

These three definitions point to the inherent problems with catheter positioning. In Figure 1 (left) we show an optimum x-ray image of a patient with a cerebral aneurysm where contrast agent has been injected to highlight the arteries for guiding the procedure. This type of imaging, however, results in a two dimensional projection of a three dimensional network. As a consequence, the surgeon is often uncertain which way to navigate the catheter. Furthermore, contrast agent can not be used continuously because of toxicity issues, so often the surgeon is unable to even see the arterial network. The illustration in

Figure 1 (right) shows a catheter procedure now being performed to eliminate the aneurysm. In this procedure a catheter is navigated into the neck of the aneurysm and embolizing coils (typically platinum coated with thrombolytic agents) are inserted into the aneurysm to initiate thrombus (clotting). This is currently a very difficult procedure, and often takes hours of manipulation to accurately position the catheter.

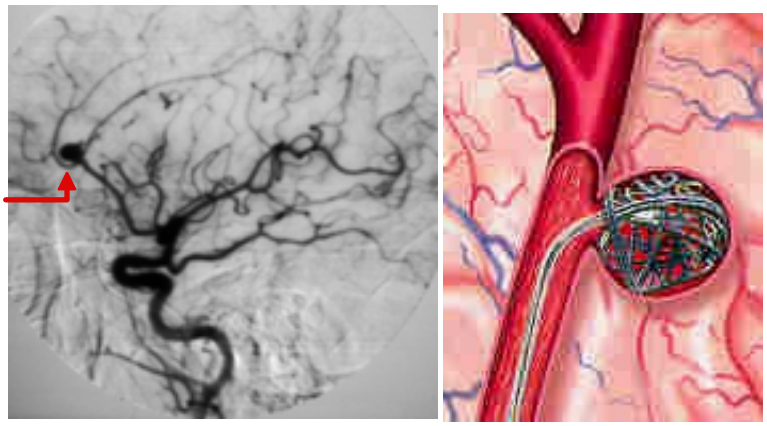

Figure 1. Angiogram showing cerebral aneurysm and an illustration showing the catheter procedure for inserting embolizing coils.

Physicians who perform catheter-based procedures have emphasized that if a compact catheter could be produced that offers local imaging and active control capabilities to guide and position the distal end of the catheter, procedures such as the one described above would be quicker, less traumatic and have a much higher rate of success. Some of the physicians we have consulted with on this project include L.N. "Nick" Hopkins, MD, Chairman and Professor Department of Neurosurgery and Radiology SUNY-Buffalo; Timothy A. Chuter, MD, Assistant Professor of Surgery Deptartment of Vascular Surgery UC San Francisco Medical Center; Chip Jungreis, MD, Associate Professor Department of Interventional Radiology University of Pittsburgh Medical Center; and Bruce McAuley, MD Interventional Cardiology Sequoia Medical Center Redwood City, CA.

Over the past three years, we have applied expertise in optical and ultrasonic imaging, microfabrication, and modeling from LLNL's Lasers and Engineering Directorates toward the development of next generation catheter technologies. The objective of this project was to enhance the physician's navigational abilities by producing a compact catheter that offers imaging and active control to guide and position the distal end. In addition, this technology has the potential for noninvasive or minimally invasive imaging of explosives and weapons systems. Figure 2 shows a conceptual illustration of the advanced imaging catheter.

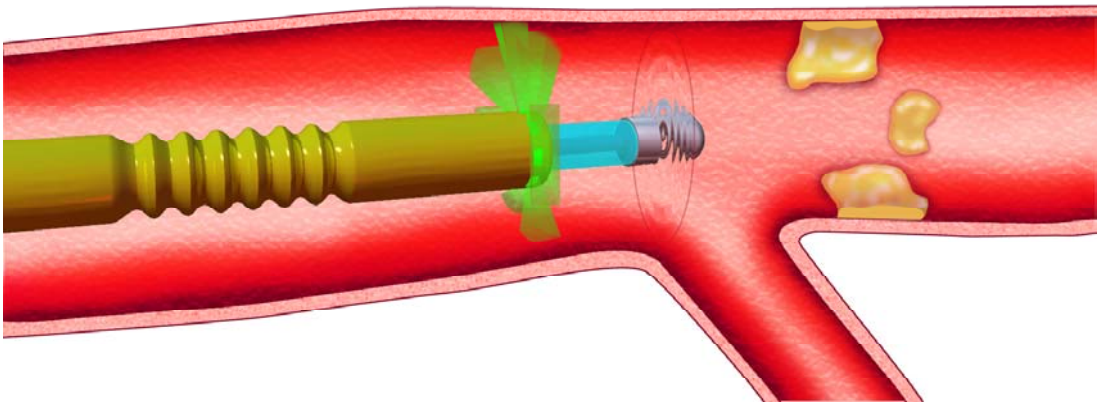

Figure 2. Illustration of advanced imaging/steerable catheter with therapy device extending past the radially imaging fibers (green light).

This project, initiated in FY98 within Laser Programs and funded through an LDRD-ER, resulted in the successful *in vitro* imaging of arterial walls using a miniaturized optical coherence tomography probe. In FY99 we extended this work to tackle two key areas in the development of the next generation of catheters. These were 1) miniaturize and multiplex optical coherence imaging technology to allow video rate imaging, and 2) develop fabrication technology to economically embed (or extrude) optical fibers within the thin polymer wall of a catheter. In FY00, we developed materials and techniques for incorporating active control into the distal end of the catheter, experimented with ultrasound for forward imaging, and focused on specific surgical applications. Collaborating with physicians at the University of California, San Francisco (UCSF), and Davis (UCD), we observed several catheter-based procedures and discussed how an articulating, imaging catheter could improve their patient outcomes. Prototype devices incorporating optical fibers for imaging, and shape-memory alloy (SMA), shape-memory polymer (SMP), and hydraulic actuation mechanisms were fabricated and tested. In this final report, we document the progress made toward developing advanced catheter technology. In all, we have transferred two devices to industry which have already generated licensing revenues, co-authored 31 papers, and produced 28 invention disclosures in this and related technologies.

Accomplishments

Optical Coherence Tomography

Optical coherence tomography (OCT) is a non-invasive, non-contact optical technique for imaging through highly scattering media. The technique uses a bright, low coherence source as part of a Michelson interferometer to accurately measure the backscattered light as a function of depth into the media. A schematic of the OCT system including the key components is shown in Figure 3. The super luminescent diode source has a broad spectral width (47 nm) that results in an axial spatial resolution in free space of ~17 microns (i.e. limited by longitudinal coherence length). The light is scanned axially through the media by varying the optical pathlength of the reference arm. Intensity modulation associated with interference between the light from the sample and reference

arm reflections (heterodyning) occurs only when the optical pathlengths of the two arms are matched with the coherence length of the source. The use of a heterodyne detection scheme makes OCT systems remarkably sensitive, with signal to noise ratios over 100 dB. The use of OCT in biological media was pioneered by James Fujimoto at MIT for imaging the human retina[1]. More recently, this group has presented OCT images of the circulatory system[2].

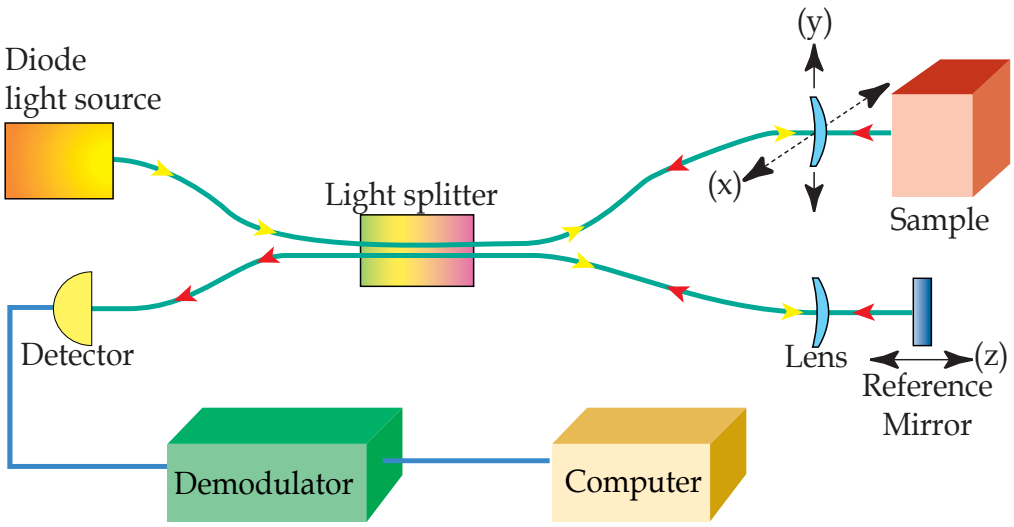

Figure 3. Schematic of fiber optic OCT system.

A cross-section of the original concept for the OCT-integrated catheter is shown in Fig. 4. The target length of the catheters was two meters long. The fibers are extruded in the walls of the catheter, so as to leave the central portion available for other diagnostic or therapeutic devices. Light is propogated down the fibers, focused using a GRIN lens, and transversely deflected using a mirrored cube.

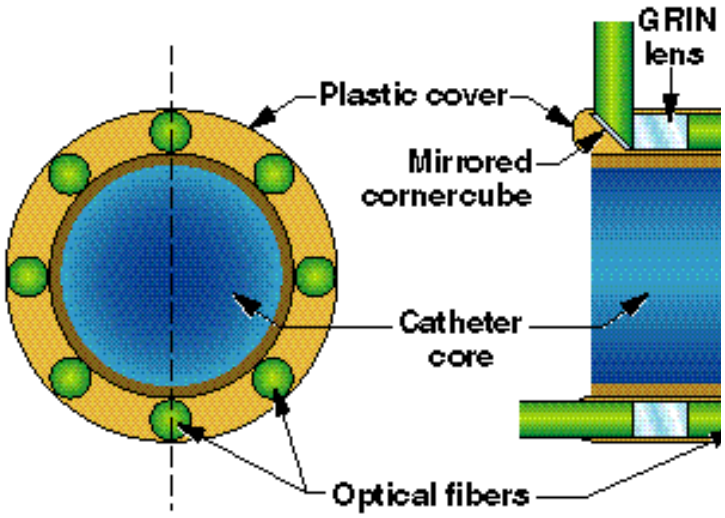

Fig. 4: Original concept for extruded catheter depicting necessary optics for OCT imaging technology. The side view (right) for illustration purposes shows both a side-firing fiber (top) and a forward firing imaging fiber (bottom).

During the course of the project, we demonstrated an optical coherence tomography (OCT) imaging system that gives us the ability to acquire 8 fiber images at 10 Hz, which is adequate for a practical medical device. The initial prototype catheter included a large rack-mounted optical and electronic system, which was replaced by a compact (18" x 18" x 3") fiber optic system with improved reproducibility. In Fig. 5, we show an end view of a polymer tube that was used to create the prototype OCT imaging catheter. The tube is 1.7 mm in diameter and has 0.2 mm diameter holes in the wall. We demonstrated that single mode optical fibers can be threaded into the wall of a 2 meter long section which meets the requirement for a device. We also have acquired, set-up, and tested a polymer extrusion machine for making tubing with embedded optical fibers as an alternative approach. Side imaging optical fibers have been developed which eliminate the need for the optical corner cubes which were required in the original design, thereby significantly reducing manufacturing costs.

Figure 5: Multi-lumen polymer tube for catheter prototype.

In FY98 a single fiber OCT system with a 250 µm diameter GRIN lens and a 250 µm corner cube was built and tested in an *ex vivo* apparatus. A test-bed apparatus was constructed for inserting the fiber optic probe into arteries containing flowing water or blood. By rotating the single fiber probe 360° in the center of the artery, we have generated ultra-high resolution (10 µm) images of the arterial walls *in situ* with flowing water (Fig. 6). We have also made significant improvements to the OCT system, increasing the sensitivity of the system by a factor of 30. This allows us to penetrate 2-3 mm into biological tissue such as arteries.

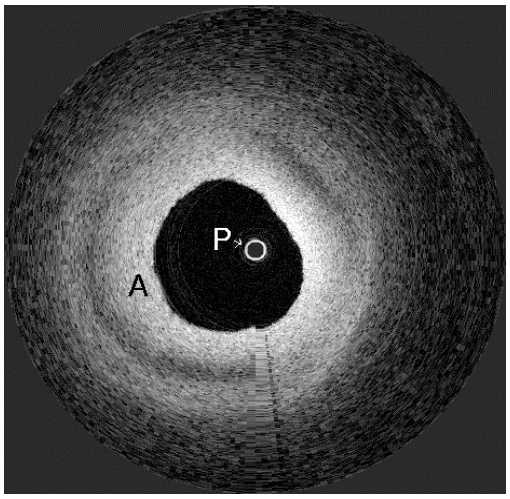

Figure 6: Image of an artery using OCT imaging. Point P indicates the position of the OCT probe, and A indicates the arterial wall. The image shown is 7 mm across, and the probe diameter is 250 microns.

In FY99, we demonstrated an OCT imaging system that operates at 50 scans/s, 10 times faster than our previous system. We also significantly improved the design of the optics at the distal end of the catheter, making 150-µm-diam probes feasible while significantly reducing manufacturing cost and enhancing robustness. We have demonstrated OCT imaging with 250-µm-diam probes deployed both through the center of a catheter and incorporated into the catheter wall. Embedding the optical fiber in the wall leaves the

central lumen of the catheter available for a medical device. An image obtained from a 250-µm-diam probe incorporated in the wall of a 1.6-mm-diam catheter tubing is shown in Fig. 7. This figure demonstrates successful imaging of the artery's walls and of a metal wire outside the artery.

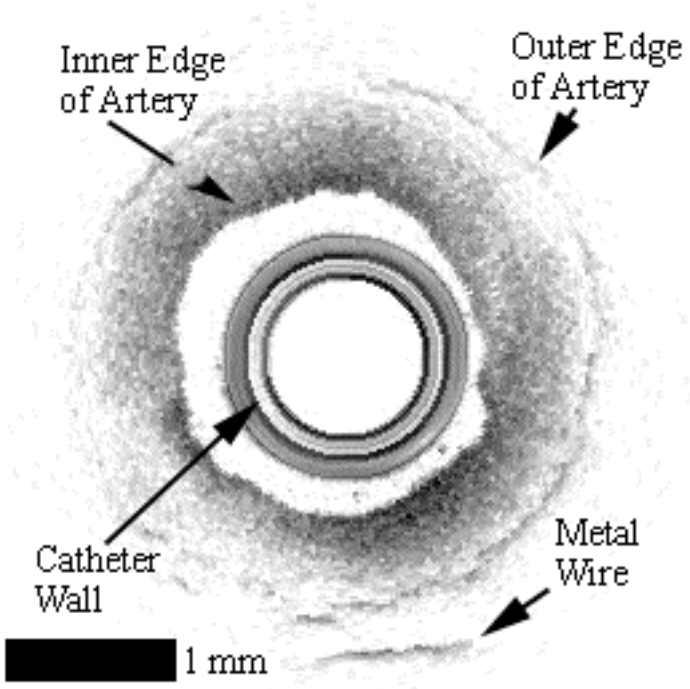

Figure 7. Optical coherence tomography (OCT) image of a porcine artery, generated from a 250-µm-diam probe embedded in the wall of a catheter.

As part of an NIH funded proposal the LLNL OCT team developed a state of the art OCT system and applied it to imaging of structures in the oral cavity[3 4 5 6 7]. The team demonstrated the potential of polarization sensitive optical coherence tomography (PS-OCT) as a non-invasive, *in vivo* detection method. The technique was applied to detection and characterization of early, incipient caries lesions. PS-OCT generates cross-sectional images of biological tissue while measuring the effect of the tissue on the polarization state of incident light. Clear discrimination between regions of normal and demineralized enamel is first shown in PS-OCT images of bovine enamel blocks containing well-characterized artificial lesions. High-resolution, cross-sectional images of extracted human teeth are then generated that clearly discriminate between the normal and carious regions on both the smooth and occlusal surfaces. Regions of the teeth that appeared to be demineralized in the PS-OCT images were verified using histological thin sections examined under polarized light microscopy. The PS-OCT system discriminates between normal and carious regions by measuring the polarization state of the back-scattered 1310 nm light, which is affected by the state of demineralization of the enamel. Demineralization of enamel increases the scattering coefficient, thus depolarizing the incident light. This study shows that PS-OCT has great potential for the detection, characterization, and monitoring of incipient caries lesions.

OCT Simulations

In conjunction with the experimental work, we also developed the capability to model OCT imaging[8]. As in any new imaging modality, physicians have expressed the need to correlate OCT images with tissue properties and conventional histology. Interpretation of OCT images can be complicated by the effects of multiple scattering and tissue birefringence. Very little modeling of OCT imaging has been performed up to now. We modified existing Monte Carlo photon transport codes to track the phase and path length of photons propagating through biological tissue and an OCT imaging system. In Fig. 8 we show the predicted OCT signal from a single imaging fiber in an artery filled with blood. The results show the rapid decay in photon signal propagating away from the fiber surface due to the high scattering coefficient of blood. The artery wall is identified by a jump in the observed signal attributable to increased scattering. The results are in good agreement with data collected in previous animal trials.

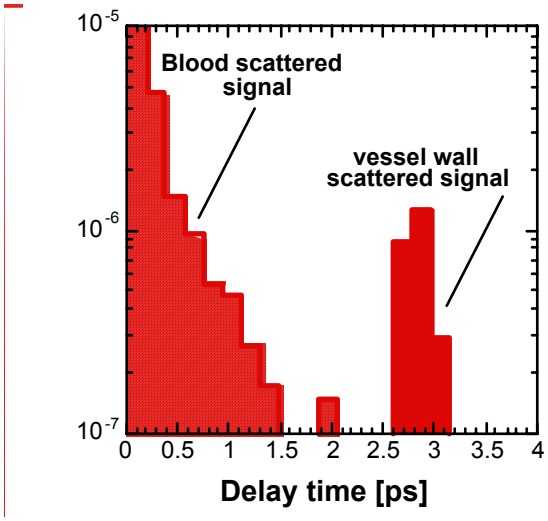

Figure 8. Predicted OCT signal from a single imaging fiber in blood-filled artery.

Catheter Articulation

In minimally invasive catheter procedures the objectives are first to navigate the catheter to the correct site, second to perform a therapy using some medical device, and finally to confirm that the therapy has been successful. With existing catheters, x-ray radiography is used to guide the device, monitor therapy and evaluate treatment. Pushing and pulling are used to position the distal tip. The problems are

1. X-ray radiography only gives the surgeon a two-dimensional projection which is often difficult to interpret and requires injecting contrast agent;
2. Local imaging techniques such as intravascular ultrasound cannot be performed continuously during the therapeutic procedure, requiring removal of the medical device from the catheter in order to insert the imaging device. This wastes time, increases costs, and limits surgical precision;
3. Accurate positioning by pushing and pulling is very difficult and time consuming;
4. Surgeons have little or no feedback about catheter status.

The Advanced Catheter Project Team met with Dr. Kirk O'Hanian, an interventional radiologist at the UC Davis Medical Center. The primary topic of discussion was how to improve the pushability, torquability and trackability of catheters during interventional procedures. Dr. O'Hanian mentioned that the most difficult problem to overcome during these procedures is the friction encountered between the catheter and the vessel walls when traversing tortuous vessels to get to a therapeutic site. Attempts had been made to make catheters more lubricious but friction still plays a major role in positioning of the catheter tip. The vasculature -- especially the neurovasculature -- is extremely tortuous, forcing the catheter to follow several bends and turns before reaching its target destination (see Fig. 1). At times, abrupt turns into branching arteries are required. As a result, frictional effects between the catheter and vessel wall lead to a deterioration of catheter tip maneuverability and control as more and more of the catheter is fed into the body. Static friction causes the catheter tip to bind, even when guide wires are used, which in turn causes the catheter to bunch up. We conceived of four potential solutions to this problem:

- Variable modulus catheter. By producing a catheter with controllable variable modulus, portions can be made stiff while others are selectively made compliant to enhance maneuverability. Approaches include polymer-based catheters that have a temperature sensitive modulus, and catheters with shape memory film elements embedded in the wall. Energy could be selectively delivered to segments of the catheter curved beyond a critical radius using optical fibers that leak light when bent. Another approach is to inject cold saline solution into a catheter formed from a polymer having a temperature-controlled modulus. The catheter could be made entirely of the temperature-sensitive material, in which case a variable length of the catheter could be stiffened, depending on flow rate of the cold solution, starting at the proximal end. Alternatively, the catheter could be constructed of different materials, such that only select regions would be transformed by the temperature change.
- Catheter with vibrational mode. If the catheter can be made to vibrate in regions where it is binding, static friction will be overcome, allowing for eased advancement of the catheter. We will investigate polymeric piezoelectric materials and catheters with embedded piezoelectric materials for this application. Opto-acoustic transduction is another potential solution to this problem, with the advantage of optically-delivered power.
- Inch-worm catheter. Segments of shape memory alloy can be embedded into the catheter sidewall and heated in succession to induce a peristaltic, rippling effect. This approach could be used to overcome static friction, or possibly even for self propulsion of the catheter tip. Another approach is to use three balloon-type elements at the catheter tip, which, when inflated in succession, would advance the catheter tip using a (1)grab-(2)advance-(3)grab-(1)release… sequence. This device could be actuated either hydraulically or thermopneumatically.
- Catheter with articulated tip. Producing a steerable catheter would greatly reduce static friction and potential snags in the most vulnerable region: the catheter tip.

Incorporation of active materials such as shape memory alloys into the catheter wall is the key to producing such a device.

One concept for achieving localized modulus control, catheter articulation, and a vibrational-mode catheter was to embed thin film shape memory alloy (SMA) ribbons within a polymer matrix (see Fig 9). LLNL has developed a unique capability for sputter-depositing nickel-titanium-copper SMA films that are ideally suited to *in vivo* medical applications.[9] Unlike typical NiTi SMA alloys, LLNL's NiTiCu films have thermo-mechanical properties that are insensitive to compositional variations. Moreover, the films begin their transformation just above body temperature and have a narrow hysteresis width (8 degrees compared to 40 for NiTi), and therefore require minimal power input for actuation. Thorough mechanical characterization has proven these films to be highly ductile, and capable of sustaining stresses greater than 400 MPa and strains up to 8% with no observable plastic deformation after shape recovery.[10 11]

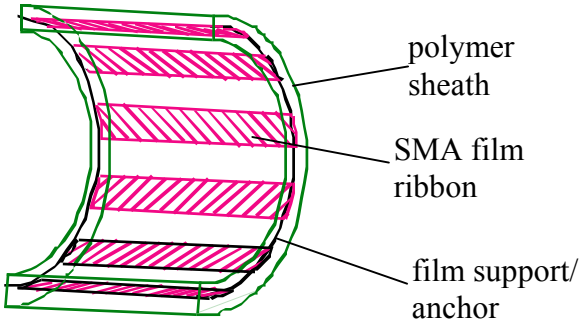

Figure 9: Shape memory film ribbons embedded in a polymer sheath

Shape memory alloys and pneumatic actuation were both investigated experimentally. The pneumatic or hydraulic solution takes advantage of high-pressure pulses of gas or liquid sent through the sub-lumens in the wall of a long catheter. This causes a slight ballooning of the pressurized sub-lumen and a moment is created down the length of the catheter by a simple material expansion. This invention is detailed in the disclosure IL-10684: A Vibrating Catheter to Reduce Static Friction Effects. This solution was explored and the initial concept was proven with pneumatic valves operating up to 50 psi, but sufficiently large displacements were not achievable. The second solution that was explored utilized shape memory alloy fibers to send standing or traveling wave patterns down the catheter with wavelength on the scale of 1 inch. This actuation method proved to yield much higher moments and motions in the catheter in proof-of-concept mockups.

Another approach we investigated for producing localized motions was to embed a shape memory alloy spring within a shape memory polymer catheter tip (Fig. 10). Heating the composite device just above the SMP transformation temperature causes it to expand and lengthen; heating above the SMA transformation temperature causes it to contract, enabling advancement of the tip when linking them end-to-end and actuating peristaltically. By fabricating and testing a 1-in.-long, 0.16-in. OD, 0.08-in. ID, hydraulically actuated, molded silicone catheter tip, we demonstrated repeatable 90-

degree bending. In addition, a fluid-filled, 6 mm-diameter polymer bellows was shown to increase in length 12 mm when heated by a laser.

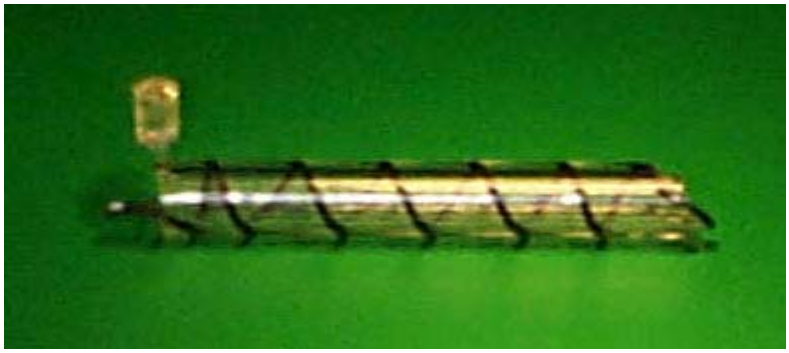

Figure 10: Shape memory alloy/shape memory polymer composite spring-tube actuator to create extensional translation

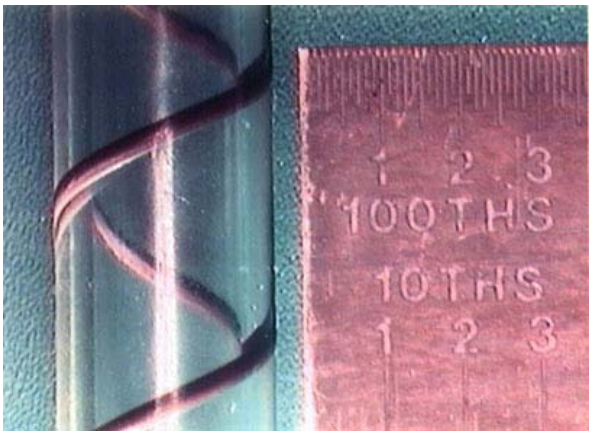

Figure 11: Close-up of shape memory alloy/shape memory polymer composite spring-tube actuator to create extensional translation

Forward-Looking Ultrasound

Using experiments and numerical simulations, we investigated forward-looking ultrasound as a potential aid in guiding a needle during an intravascular liver-bypass procedure known as transjugular intrahepatic portosystemic shunting (TIPS). The objective was to study the feasibility of a simple depth-ranging device, simulating a single element PZT transducer placed at the end of a catheter-guiding needle. Harder tissues reflect more acoustic energy compared to blood-filled veins, thus enabling navigation through a diseased liver.

To demonstrate the principle, a single element, commercially available circular transducer was placed in a water bath aiming at a vessel-mimicking tube. A pulser/receiver drove the 5MHz ultrasound transducer. This device delivered electrical pulses to the transducer, which converted the electrical signal to acoustic energy. After

the initial pulse (t=0) the receiver amplified the return signal (reflections) coming from the transducer and output the signal to an oscilloscope. The oscilloscope stored the signal for download (Fig. 12).

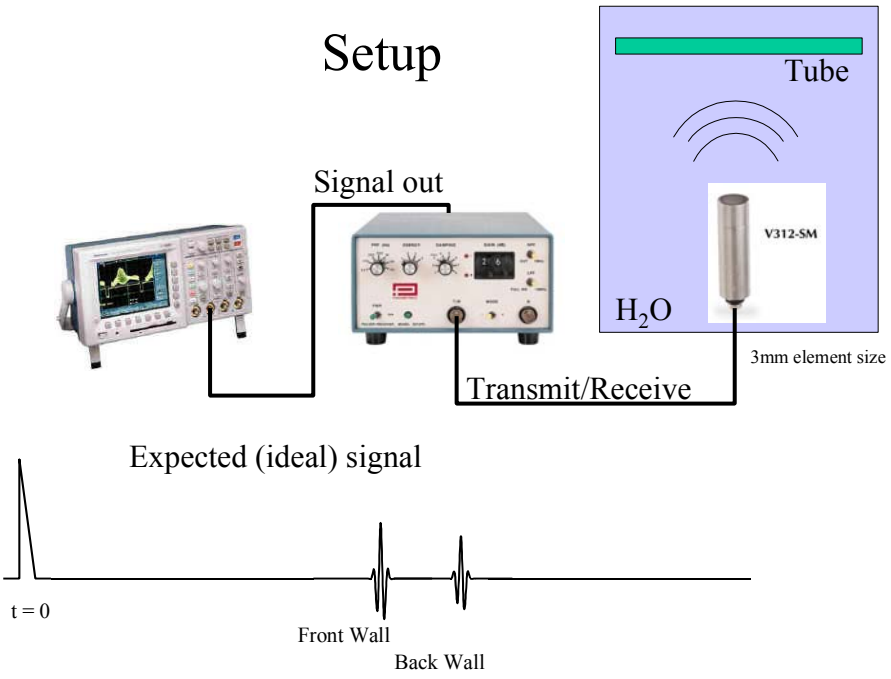

Figure 12: Experimental setup for forward-looking ultrasound proof of concept.

Resolution can be determined by calculating the width of the radiated acoustic beam shape and the length of the pulse (Fig. 13). There are three resolutions to be determined since it is a 3-Dimensional problem. For reference purposes we define a coordinate system with respect to the element orientation. The X-axis is along the width of the element, the Y-axis is along the height and the Z-axis is the distance away from the element or depth. The size and shape of the element determine resolution in the width and height dimensions. The bigger the element the narrower the beam at a certain distance. Smaller elements have a larger spherical spreading over which the energy is distributed.

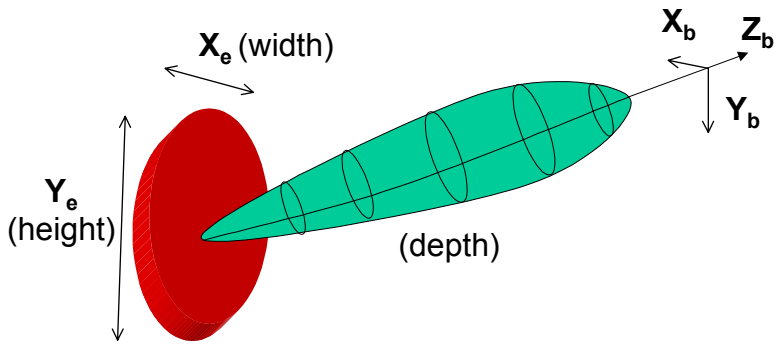

Figure 13: Axis definition, element and beam coordinate system.

The acoustic pulse length in time determines resolution in depth. Shorter pulses have higher resolution. The carrier frequency and the bandwidth of the transducer determine the length of the pulse. High frequency, broadband transducers have high resolution. However, high frequencies are attenuated faster in tissue and broadband transducers are complex and costly to manufacture. A 5-10 MHz carrier frequency with 50% bandwidth is a reasonable trade-off for this application based on current medical ultrasound applications.

The Rayleigh criterion is used to calculate resolution. According to this criterion, two intensity distributions are resolved when the maximum of one distribution overlaps the first minimum in the diffraction pattern of the second distribution. Figure 14 indicates two spots that are barely resolved according to the Rayleigh criterion. The solid lines represent the diffraction patterns of the individual distributions. The dotted line represents the sum of the two distributions. This resolution criterion can be applied to the beam profile and the envelope of the RF signal pulse to determine the resolution in width and height and in depth respectively.

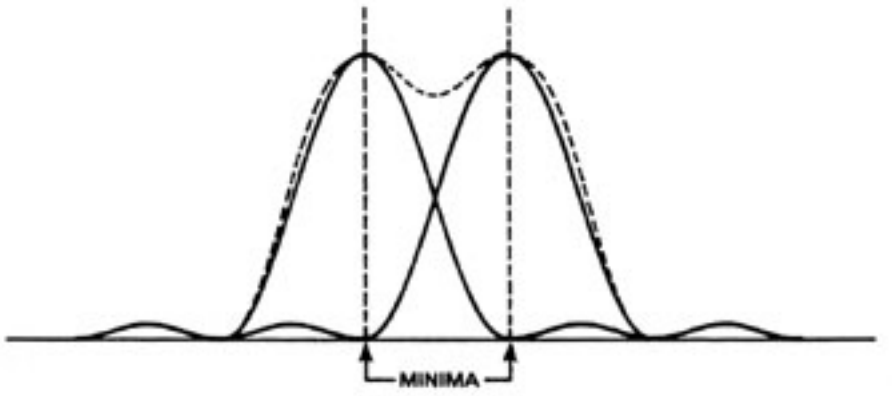

Figure 14: Rayleigh criterion for resolution.

To study the effect of size and shape of the acoustic field generated by the transducer a numerical study was performed. This enables choosing the correct design parameters for optimizing the space requirements and improving the imaging resolution. Three different configurations were chosen in this study (see Fig 15) – a half circle element, a full circle and a cylindrical shape element. The transducer has to be integrated with a needle in a single catheter. The half circle shares the opening with the needle, the full circle requires a double barrel design and the cylindrical design allows inserting a needle through the center of the element.

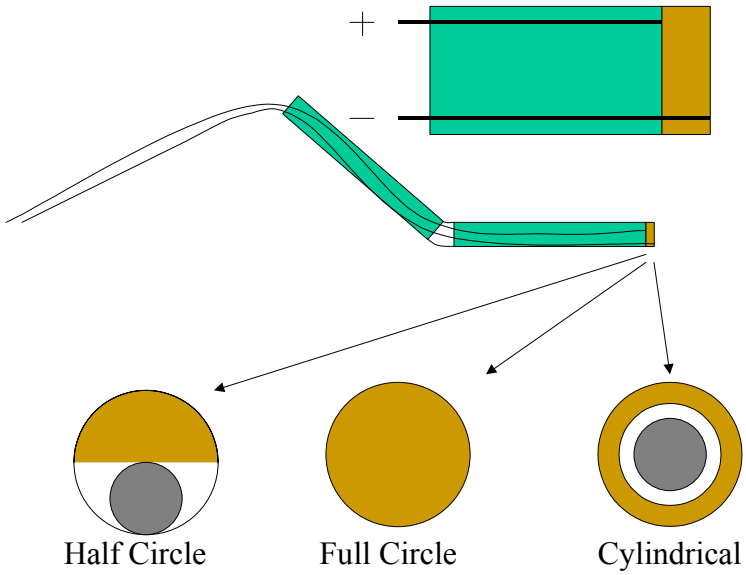

Figure 15: Three configurations for active transducer material at the catheter tip.

Figure 16 shows an RF signal from the transducer aiming at the vessel-mimicking rubber tube. The time scale is converted to distance using 1540 mm/sec for the speed of sound in water. For scaling purposes the initial pulse has been removed from the signal (at t=0, 0 distance). The first interface the acoustic wave encounters is the front wall of the tube and a large amount of energy is reflected back to the transducer. The tube is positioned approximately 40mm from the transducer. A second, much smaller reflection can be seen coming from the back wall of the tube near 75 mm. This illustrates the ability to measure the distance to the vessel and the size of the vessel.

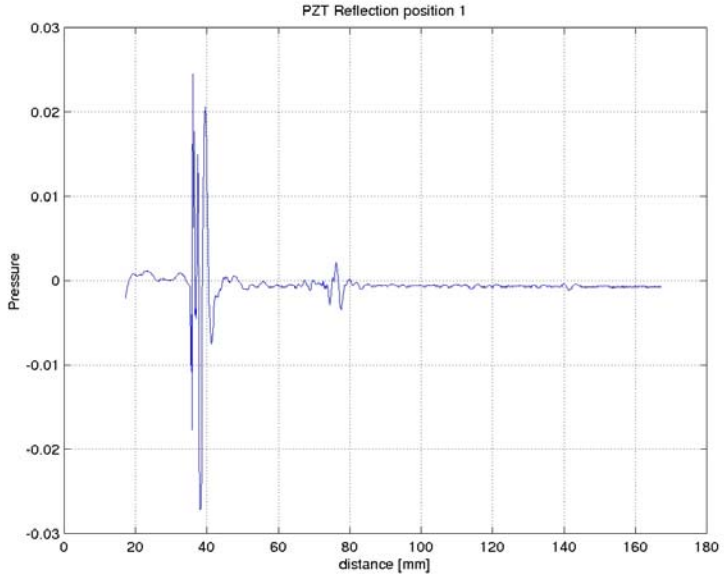

Figure 16: Measured RF signal from a soft rubber tube. The large signal at 40mm distance from the transducer is the front wall of the tube, the smaller signal at 75mm is the back wall of the tube. The tube diameter is approximately 35mm.

To simulate the acoustic beam pattern of each transducer, three different models were constructed. Each model consists of small square units from which the acoustic response was calculated similar to the finite element method (see Fig. 17).

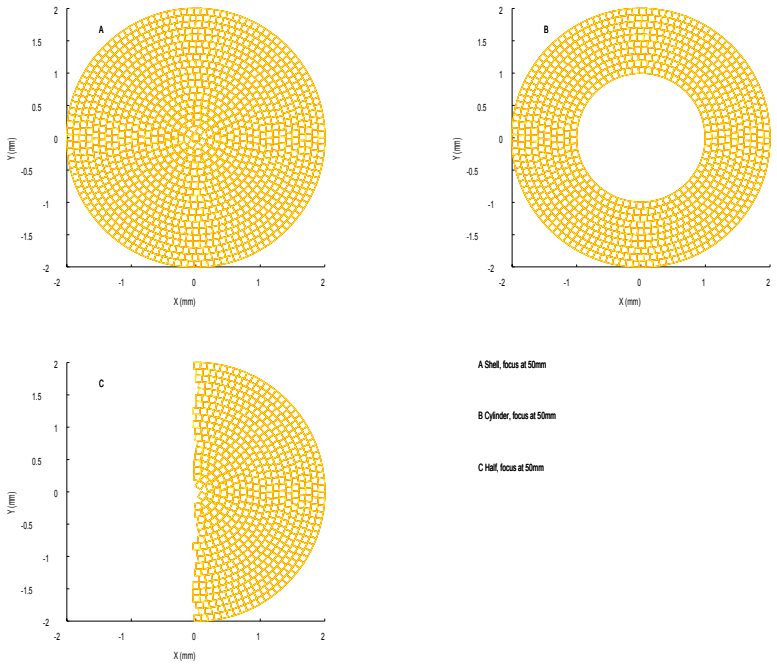

Figure 17: Each transducer model consists of numerous square elements.

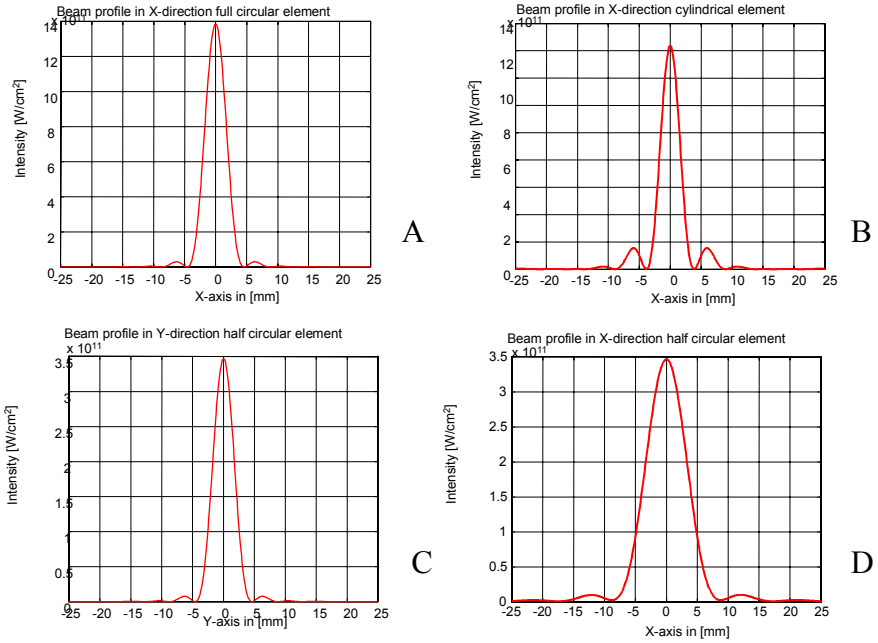

Figure 18: Beam width calculations at 25mm distance from the transducer for A: the full circle model, B: the cylindrical model, C: the half circle in the Y dimension and D: the half circle in the X dimension.

Figure 18A shows the beam cross section from a circular element measured 50mm from the front of the transducer. The full-width-half-max beam width is approximately 5mm, which is equivalent to the lateral and azimuth resolution. Figure 18B shows the beam width of the cylindrical transducer. The beam width is similar to the circular transducer but an increase in side lobes is observed due to the reduced aperture surface. Figure 18C shows the beam width of the half circle element. As expected the profile is identical to the profile of the full circle in the Y-dimensions. The X-dimension (Fig 18D) shows a wider beam due to the smaller element size, with a corresponding reduction in resolution in the X-dimension. The full circle is the preferred configuration since it offers low side lobe levels and the best resolution in all dimensions.

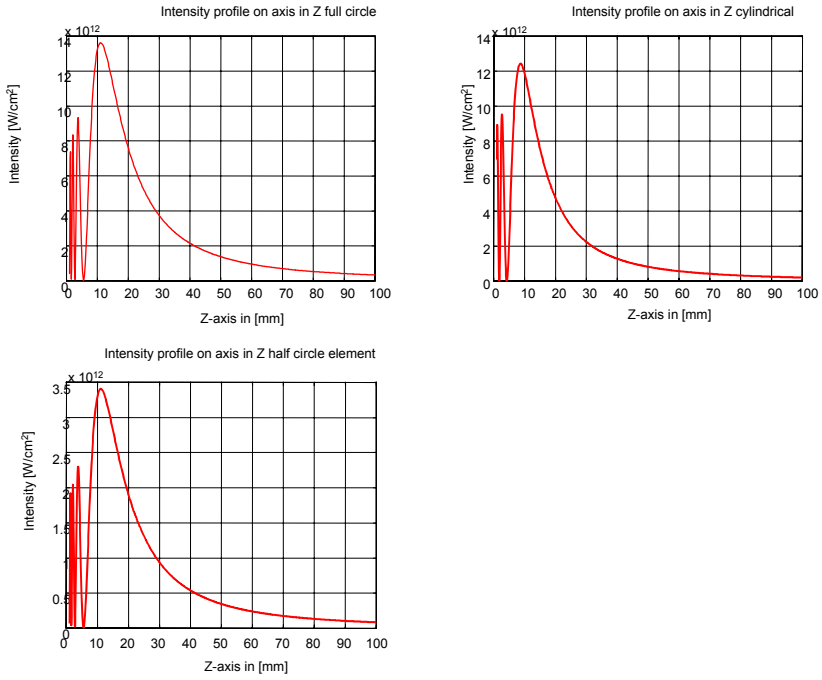

Figure 19: Depth profile for all three transducer configurations.

Figure 19 shows the intensity profile for all three transducer configurations. The profiles are very similar and show the characteristic near field and far field transition after which the intensity falls off as 1/distance from the transducer. This figure tells us that imaging in the near field, closer than 10mm can give erroneous results due to local oscillations in the acoustic field. These calculations were done using single frequency continuos wave simulations, which can be considered worst case for two reasons. First, side lobes will be reduced in broadband applications because the multiple frequency components place the side lobes at a different location, near the main lobe, resulting in a lower, average side lobe level. For the same reason, in broadband applications local oscillation will be weaker in the near field.

As stated earlier, the full circle transducer predicted best results in beam profile studies with respect to side lobe levels and resolution. The next step was to determine the size of

the transducer for the appropriate resolution and depth requirements. Four different size circular transducers – 1, 2, 4 and 6 mm – were compared. The total number of square element calculation units was kept the same. Multiple frequency components were used to make the beam profiles closer to their realistic shape. A center frequency of 5MHz with 50% bandwidth was chosen in this case.

Figure 20 shows the beam profiles in the X-dimension at 25mm distance for transducers with increasing diameter. As expected, the beam narrows with increasing diameter. In the last case (6mm diameter) the beam profile seems to widen and take a different shape. This is due to the position where the beam profile is measured. With the help of Fig. 19 we see that in the 6 mm case, a distance of 25 mm is located in the near field of the transducer. As seen in Fig. 21, the larger the element the farther the near field extends from the transducer. The peak intensity (far field transition) is located at a greater distance from the transducer. Near field imaging should be avoided because of oscillation in the beam pattern. From these results we see that a trade-off has to be made: a larger element will give a narrower beam and thus higher resolution, but a large element makes imaging close to the transducer difficult.

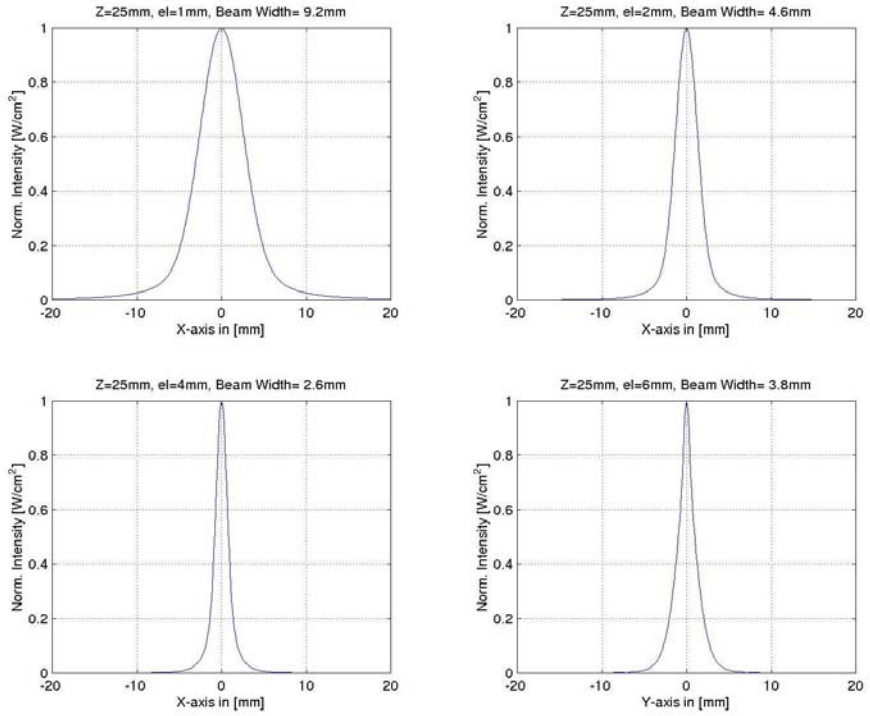

Figure 20: X-dimension, (in width) beam profile for circular transducer with increasing diameter 1, 2, 4 and 6 mm.

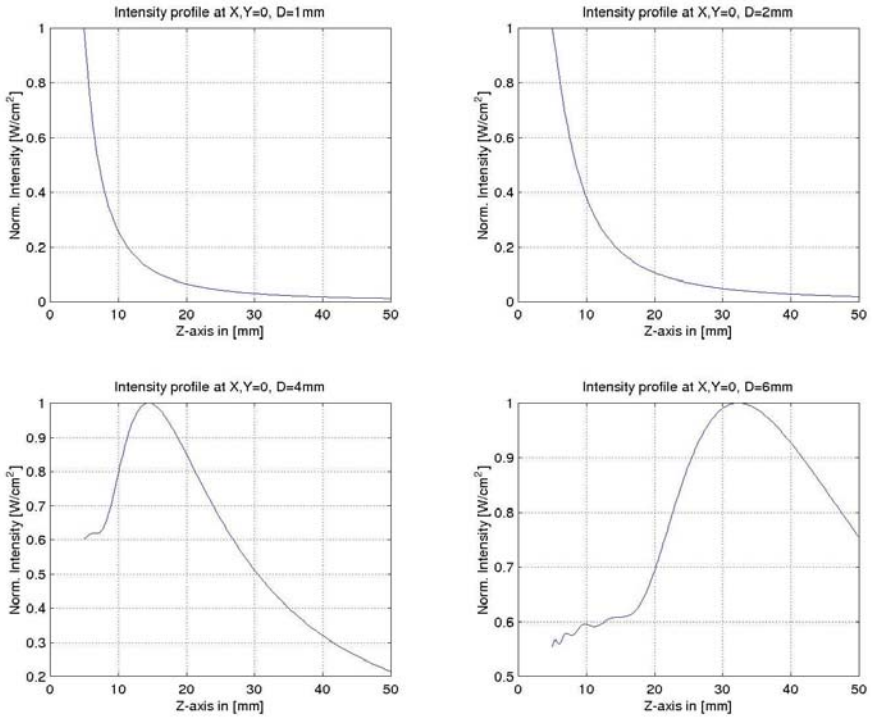

Figure 21: Z-dimension (in depth) beam profile for circular transducer with increasing diameter.

Preliminary proof-of-concept measurements in a water tank indicate the possibility of measuring vessel distance and size with a single element transducer. Numerical simulations were used to study design parameters such as size and configuration of the transducer to optimize and predict measurement resolutions. A nominal frequency near 5MHz was suggested to enable adequate acoustic penetration into tissues and obtain good resolution. To allow imaging close to the transducer element sizes smaller than 3 mm in diameter should be considered to avoid near field oscillation. A 3mm element will give a spatial resolution in the width and height dimension of about 3.5mm.

Conclusions

Several aspects of an advanced imaging catheter were demonstrated during the course of this project. Optical coherence tomography was shown to be an effective technique for imaging within the vessels. An OCT catheter was constructed with optical fibers embedded in the catheter sidewalls, leaving a large internal lumen open for introducing other therapeutic devices. Simulations of OCT in blood were used to estimate penetration depth and imaging capability. Shape memory alloy, shape memory polymer, and hybrid devices were investigated for catheter articulation. Hydraulic actuation was also explored. Experiments and numerical simulations were performed to demonstrate that forward-looking ultrasound is an attractive method for guiding catheters.

References

[1] D. Huang, et al., *Optical Coherence Tomography,* Science **254**,1178(1991). E.A. Swanson, et al., Optics Letters **17**,151(1992).

[2] G.J. Tearney, S.A. Boppart, B.E. Bouma, M.E. Brezinski, N.J. weissman, J.F. Southern, and J.G. Fuijimoto, *Scanning single-mode fiber optic catheter-endoscope for optical coherence tomographys,* Optics Letters **21**,541(1996).

[3] B.W. Colston Jr., M.J. Everett, L.B. Da Silva, L.L. Otis, P. Stroeve, H. Nathel*, Imaging of hard and soft tissue structure in the oral cavity by optical coherence tomography*, Applied Optics, Vol 37 (1998) 3582. UCRL-JC-127487.

[4] MJ. Everett, U.S. Sathyam, B.W. Colston Jr., L.B. Da Silva, D. Fried, J.N. Ragadio, and J.D.B. Featherstone, "Polarization Sensitive Optical Coherence Tomography Detection Method," presented at Early Detection of Dental Caries III, Indianapolis, IN, May 1999. UCRL-JC-134114.

[5] M. J. Everett, U. S. Sathyam, B. W. Colston, L. B. Da Silva, D. Fried, J. N. Ragadio, and J. D. B. Featherstone, "Non-Invasive Diagnosis of Early Caries with Polarization Sensitive Optical Coherence Tomography," submitted to Journal of Biomedical Optics, July 1999. UCRL-JC-132683

[6] B.W. Colston, Jr., M.J. Everett, U.S. Sathyam, L.B. DaSilva, and L.L. Otis, "Imaging of the Oral Cavity Using Optical Coherence Tomography," submitted to a book entitled Monographs in Oral Health, December 1998. UCRL-JC 135908.

[7] M.J. Everett, B.W. Colston, L.B. DaSilva, and L.L. Otis, "Fiber Optic Based Optical Coherence Tomography (OCT) for Dental Applications," Fourth Pacific Northwest Fiber Optic Sensor Wrkshop, Portland, Oregon, May 1998. UCRL-JC-13698.

[8] Peter Amendt, K. Estabrook, M. Evecem R.A. London. D, Maidand, G. Zinmwtmut, B. Colston, L. da Silva and U. Sathyamr, *Monte Carlo simulations of arterial imaging with optical coherence tomography*, presented at SPIE/BIOS Conference on Gastrointestinal Surgery, San Jose, CA, January 22,2000, UCRL-JC- 135024.

[9] P. Krulevitch, A.P. Lee, P.B. Ramsey, J.C. Trevino, J. Hamilton, and M.A. Northrup, "Thin Film Shape Memory Alloy Microactuators," *J. Microelectromechanical Systems*, **5** (1996) 270.

[10] Kirk P. Seward, Peter Krulevitch, Harold D. Ackler, and Philip B. Ramsey, "A New Mechanical Characterization Method for Microactuators Applied to Shape Memory Films," *presented at Transducers '99*, Japan. UCRL-JC-132488

[11] K.P. Seward, D.S. Nath, P.B. Ramsey, and P. Krulevitch, "Thermomechanical Characterization of Nickel-Titanium-Coper Shape Memory Alloy Films," ASTM Symposium on Mechanical Properties of Structural Films, Orlando, FL, November 1999. UCRL-JC-136906-ABS